Cyclostationary Detection of 5G GFDM Waveform in Cognitive Radio Transmission

Rohit Datta[a], Dorin Panaitopol[b], and Gerhard Fettweis[a]
[a]Vodafone Chair Mobile Communications Systems, Dresden University of Technology, Dresden, Germany.
[b]NEC Technologies (UK), FMDC Lab., ComTech Department, Nanterre, France.
Email:{rohit.datta, gerhard.fettweis}@ifn.et.tu-dresde.de, dorin.panaitopol@nectech.fr

***Abstract*—Generalized frequency division multiplexing (GFDM) is a new flexible multicarrier waveform. With the flexibility of pulse shaping techniques and a tail-biting cyclic prefix, it has very low out of band leakage. This makes this potential 5G waveform suitable for cognitive radio opportunistic access with lower interference to the adjacent legacy/primary users. Because of the per-subcarrier pulse shaping technique, the cyclostationary autocorrelation properties of GFDM produces extra correlation peaks at particular cyclic frequencies. Cyclostationary detection based on these side peaks improve the spectrum sensing of GFDM over traditional OFDM. The GFDM receiver with ICI cancellation unit mitigates the ICI for any values of the roll-off factor, and hence, increasing the roll-off factor does not impact the BER performance of the GFDM system. This paper highlights the innovative cyclostationary properties of GFDM and studies the effect of pulse shaping roll-off factors on detection performance.**

Keywords: 5G Waveform, cognitive radio, cyclostationary detection, GFDM, spectrum sensing.

I. Introduction

Available wireless spectrum is getting rare with more and more devices utilizing, and taking up this already scarce resource. New and innovative methods to intelligently use available spectrum has opened up the door for invigorative research in cognitive radio technologies [1], [2]. Apart from different cognitive radio networking topics, one of the most important research direction is towards developing flexible, multicarrier, and potential 5G waveforms, with extremely low out of band leakage to satisfy regulatory requirements [3], [4].

The multiband generalized frequency division multiplexing (GFDM) [5], [6], is a new idea for designing a multicarrier PHY. GFDM is block based multicarrier transmission scheme derived from filter bank approach, where, the transmit data of each block is distributed in time and frequency, and each subcarrier is pulse shaped with an adjustable pulse shaping filter. GFDM with flexibility of adaptive subcarrier bandwidth and carrier aggregation, can be considered as an ultra wideband (UWB) technology. GFDM is well suited for cognitive radio (CR), as the choice of pulse shaping filters makes the out-of-band leakage extremely small. GFDM also has a tail-biting cyclic prefix (CP) that increases the overall throughput of the system, and compared to filter bank multicarrier (FBMC) systems [7], [8], helps in synchronization efforts [9], [10].

This paper studies the cyclostationary properties of GFDM, and utilizes it for feature detection of GFDM cognitive radio signal. We use spectrum sensing for the protection of opportunistic users and assumes that incumbent users are protected using the geo-location database approach. More complex than the classical energy detector (ED) [11], the cyclostationary detector (CD) [12], [13], exploits the cyclostationary features of the signal. GFDM being a novel flexible waveform, researching its cyclostationary properties have only just begun [14], [15]. Based on different GFDM parameters, like the pulse shaping roll-off factor or the length of the CP, the cyclostationary property changes. In this paper we have analyzed the effects of these GFDM parameters on detection probabilities. Generalized likelyhood ratio test (GLRT) [16], [17], has been performed for one non-zero cyclic frequency which characterizes the GFDM CAF structure, and differentiates it from noise. The numerical results show a comparison between different detection results for different values of roll-off factor.

The remainder of the paper is structured as follows: Section II describes the GFDM transmitter model, Section III also shows a new receiver design together with performance results, highlighting that the CP length or the roll-off factor has no impact on BER performance. Then follows a description of GFDM cyclostationary properties in Section IV. Section V describes, in brief, the GLRT detector employed, to detect GFDM cognitive radio waveform, with the conclusion in Section VI.

II. GFDM transmitter system model

GFDM is a multi-carrier modulation scheme with flexible pulse shaping. Initially the binary data is modulated and divided into sequences of $K \times M$ complex valued data symbols. Each such sequence $d[\ell]$, $\ell = 0, 1, \cdots, KM-1$, is spread across K subcarriers and M time slots for transmission. The data is represented by means of a block structure defined in equation (1) as

$$\begin{aligned}\mathbf{D} &= [\mathbf{d}_0, \mathbf{d}_1 \cdots \mathbf{d}_{K-1}]^{\mathrm{T}}, \\ &= \begin{bmatrix} d_0[0] & \dots & d_0[M-1] \\ \vdots & & \vdots \\ d_{K-1}[0] & \dots & d_{K-1}[M-1] \end{bmatrix},\end{aligned} \tag{1}$$

where $d_k[m] \in \mathbb{C}$ is the data symbol transmitted on the kth subcarrier and in the mth time slot. OFDM is a special case of GFDM, where $M = 1$, i.e. the data is spread only across frequencies and not in time.

The GFDM transmitter structure is shown in Fig. 1. In the kth branch of the transmitter, the complex data symbols $d_k[m]$, $m = 0, \ldots, M-1$ are upsampled by factor N, resulting in

$$d_k^N[n] = \sum_{m=0}^{M-1} d_k[m]\delta[n - mN], \quad n = 0, \ldots, NM-1, \quad (2)$$

where $\delta[\cdot]$ is the Dirac delta function. Consequently, $d_k^N[mN] = d_k[m]$ and $d_k^N[n] = 0$ for $n \neq mN$.

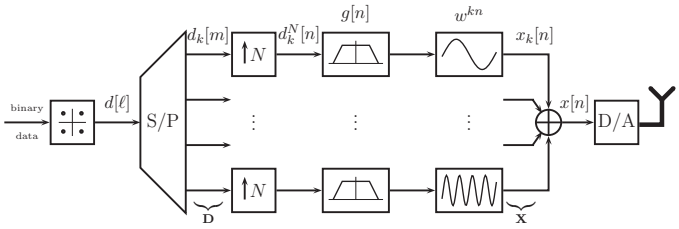

Fig. 1. GFDM transmitter system model

The pulse shaping filter $g[n]$ is applied to the sequence $d_k^N[n]$, followed by digital subcarrier upconversion. The resulting subcarrier transmit signal $x_k[n]$ can be mathematically expressed as

$$x_k[n] = \left(d_k^N \circledast g\right)[n] \cdot w^{kn} \quad (3)$$

where $\circledast$ denotes circular convolution and $w^{kn} = e^{j\frac{2\pi}{N}kn}$. Similar to equation (1), the transmit signals can be expressed in a block structure

$$\begin{aligned} \mathbf{X} &= [\mathbf{x}_0, \mathbf{x}_1 \cdots \mathbf{x}_{K-1}]^{\mathrm{T}}, \\ &= \begin{bmatrix} x_0[0] & \ldots & x_0[MN-1] \\ \vdots & & \vdots \\ x_{K-1}[0] & \ldots & x_{K-1}[MN-1] \end{bmatrix} \end{aligned} \quad (4)$$

The transmit signal for a data block $\mathbf{D}$ is then obtained by summing up all subcarrier signals according to

$$x[n] = \sum_{k=0}^{K-1} x_k[n]. \quad (5)$$

As shown in [18], [19], when all transmit samples are collected in a vector $\mathbf{x} = [x_0, \cdots, x_{K-1}]^T$, the GFDM transmitter [6] can be formulated as

$$\mathbf{x} = \mathbf{A}\mathbf{d}. \quad (6)$$

Herein, $\mathbf{A}$ is a $NM \times KM$ complex valued modulation matrix with elements based on the parameters M, K, N and $g[n]$.

The matrix $\mathbf{A}$ contains all transmit signal processing operations and is given by

$$\mathbf{x} = \mathbf{W}_{NM}^H \sum_{k=0}^{K-1} \mathbf{P}^{(\mathbf{k})} \mathbf{\Gamma}_{\mathrm{Tx}}^{(L)} \mathbf{R}^{(L)} \mathbf{W}_M \mathbf{d}_k, \quad (7)$$

where the data symbols $\mathbf{d}_k$ on the k^{th} sub-carrier are first transformed to frequency domain by multiplication with an $M \times M$ discrete Fourier transform (DFT) matrix $\mathbf{W}_M = \{w_{i,j}\}_{M \times M}$, where $w_{i,j} = e^{-j2\pi\frac{ij}{M}}$ with $i = 0, \ldots, M-1$ and $j = 0, \ldots, M-1$.

Then, tightly related to the localized non-zero coefficients of the frequency response of the pulse, the resulting frequency samples are duplicated L-fold by multiplication with a repetion matrix $\mathbf{R}^{(L)} = \begin{pmatrix} \mathbf{I}_M & \mathbf{I}_M & \ldots \end{pmatrix}^T$, which is a concatenation of L identity matrices $\mathbf{I}_M$ of size $M \times M$. This operation corresponds to an L times upsampling in time domain.

Subsequently, each sub-carrier is filtered with $\mathbf{\Gamma}_{\mathrm{Tx}}^{(L)}$, a matrix which contains $\mathbf{W}_{LMg}^{(L)}$ on its diagonal and zeros otherwise. Note that, while $\mathbf{g}$ contains NM filter coefficients, $\mathbf{g}^{(L)}$ can be downsampled by N/L and thus reduced to only LM samples, if it contains negligible filter coefficients that are zero and near-zero in frequency domain.

Finally, the k-th sub-carrier is up-converted to its respective sub-carrier frequency with the permutation matrix $\mathbf{P}^{(k)}$, which can be constructed according to

$$\mathbf{P}^{(0)} = \begin{pmatrix} \mathbf{I}_{LM/2} & \mathbf{0}_{LM/2} & \cdots & \mathbf{0}_{LM/2} & \mathbf{0}_{LM/2} \\ \mathbf{0}_{LM/2} & \mathbf{0}_{LM/2} & \cdots & \mathbf{0}_{LM/2} & \mathbf{I}_{LM/2} \end{pmatrix}^T$$

$$\mathbf{P}^{(1)} = \begin{pmatrix} \mathbf{0}_{LM/2} & \mathbf{I}_{LM/2} & \cdots & \mathbf{0}_{LM/2} & \mathbf{0}_{LM/2} \\ \mathbf{I}_{LM/2} & \mathbf{0}_{LM/2} & \cdots & \mathbf{0}_{LM/2} & \mathbf{0}_{LM/2} \end{pmatrix}^T$$

etc. with $\mathbf{0}_{LM/2}$ being an $\frac{LM}{2} \times \frac{LM}{2}$ matrix containing zero elements. Here, T denotes the transpose of the matrix. This matrix shifts and exchanges the upper and lower part of the base band spectrum of the sub-carrier onto its band pass representation.

After that, the signals of all K sub-carriers are superpositioned and the result is transformed back to the time domain with $\mathbf{W}^{NM}$.

Tail biting [20], has been applied to GFDM and this has been used to reduce the length of the CP. It is used to maintain the circular structure within each block. This tail biting concept exploits the digital implementation of the filters to perform circular convolution. $\widetilde{x}[n]$ is then passed to the digital-to-analog converter and sent over the channel.

III. GFDM RECEIVER SYSTEM MODEL

The GFDM receiver block, along with interference cancellation unit, is shown in Fig. 2. $y[n]$ is the received signal containing noise and self-ICI due to non-orthogonal GFDM subcarriers. $\hat{y}^{(i)}[n]$ is the signal without any ICI, but tainted with only noise. We have considered a perfectly synchronized GFDM receiver, and hence the cyclostationary detector does not suffer from any frequency or timing offsets.

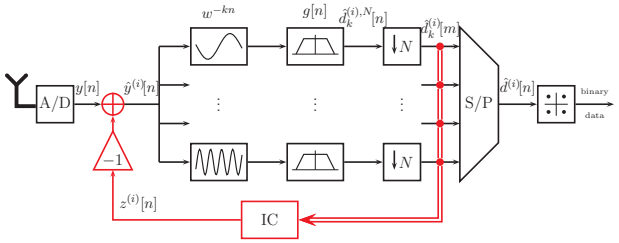

Fig. 2. GFDM receiver system model

From [6], we see that, interferences from both the adjacent subcarriers are removed simultaneously. If k is the subcarrier of interest, the data on the $(k-1)^{\text{th}}$ and on the $(k+1)^{\text{th}}$ subcarriers are $\hat{d}_{k-1}^{(i)}[m]$ and $\hat{d}_{k+1}^{(i)}[m]$.

Now, $\hat{d}_{k-1}^{(i)}[m]$ and $\hat{d}_{k+1}^{(i)}[m]$ are mapped by a detector to the constellation grid to get $d_{k-1}^{(i),e}[m]$ and $d_{k+1}^{(i),e}[m]$. The data matrix in the interference cancellation unit, $\{d_k^{(i),e}[m]\}_{K\times M}$ now has non-zero elements in rows $k-1$ and $k+1$. This is then sent to the GFDM IC block.

In the GFDM IC block, the interference cancellation signal is obtained as

$$z^{(i)}[n] = (d_{k-1}^{(i),e} \circledast g)[n]\cdot w^{(k-1)n} + (d_{k+1}^{(i),e} \circledast g)[n]\cdot w^{(k+1)n}. \quad (8)$$

$z^{(i)}[n]$ is then subtracted from the composite received signal $y[n]$ to get $\hat{y}^{(i)}[n]$. This mitigates the intercarrier interference from subcarrier $k-1$ and $k+1$.

Now the interference cancelled signal, $\hat{y}^{(i)}[n]$, is digitally subcarrier down converted, filtered with the pulse shaping filter sampled response and down sampled to get the received data symbols for the k^{th} subcarrier. Mathematically, this process can be expressed as follows

$$\hat{y}_k^{(i)}[n] = \hat{y}^{(i)}[n]\cdot w^{-kn}, \quad (9)$$

$$\hat{d}_k^{(i+1),N}[n] = (\hat{y}_k^{(i)} \circledast g)[n], \quad (10)$$

$$\hat{d}_k^{(i+1)}[m] = \hat{d}_k^{(i+1),N}[n = mN]. \quad (11)$$

For cleaning the $(k+1)$th subcarrier, data symbols from the most recent sub-iteration are used. Hence, the interference cancellation process continues and cancels out all the interference from the GFDM system, caused due to non-orthogonality of the subcarriers.

With increasing roll-off factor, α, each of the subcarriers interfere more to the adjacent subcarriers. This, in turn, causes the BER to increase, as shown in Fig. 3. The interference cancellation block, from Fig. 2, irrespective of the value of α, iteratively removes the self generated intercarrier interference.

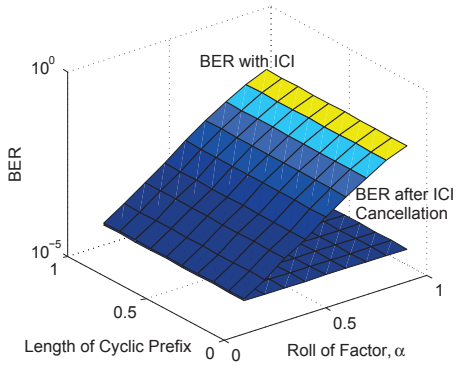

Fig. 3. BER with ICI vs. BER after ICI cancellation, as a function of different roll-off factors (α), and different normalized Cyclic Prefix lengths, for 10 dB SNR

Fig. 3 also highlights the fact that length of CP has no effect on self-ICI, i.e., the length of CP does not really matter, as opposed to what happens for OFDM. More detailed ICI cancellation and BER studies have been performed in [6]. This section highlights that BER is not impacted for different CP lengths and roll-off factor, and hence, we have exploited that in improving the cyclostationary detection performance in Section V.

IV. GFDM Cyclostationary Properties

The autocorrelation function $R_{yy}(t,\tau)$ of the received signal $y(t)$ can be represented by Fourier series expansion as

$$R_{yy}(t,\tau) = \sum_{\beta\in\psi} R_{yy}^{\beta}(\tau)\, \mathrm{e}^{(j2\pi\beta t)}, \quad (12)$$

where β, is a cyclic frequency, ψ is the entire set of cyclic frequencies, and $R_{yy}^{\beta}(\tau)$ is the Fourier coefficient, also called Cyclic Autocorrelation Function (CAF). Here, $y(t) = h(t) * x(t) + n(t)$, with white additive Gaussian noise (AWGN) denoted as $n(t)$, and where $h(t)$ is the channel. Let us clarify that the cyclic autocorrelation has been performed on $\hat{y}^{(i)}$. The CAF of the second order autocorrelation function can be written as

$$\begin{aligned} R_{yy}^{\beta}(\tau) &= \lim_{T\to\infty}\frac{1}{T}\int_{-\frac{T}{2}}^{\frac{T}{2}} y(t)y^*(t-\tau)\mathrm{e}^{-j2\pi\beta t}dt \\ &= \lim_{T\to\infty}\frac{1}{T}\int_{-\frac{T}{2}}^{\frac{T}{2}} y^*(t)y(t+\tau)\mathrm{e}^{-j2\pi\beta t}dt. \end{aligned} \quad (13)$$

The expression described by (13) could be time-discrete approximated by

$$R_{yy}^{\beta}[d] = \frac{1}{N_y}\sum_{n=0}^{N_y-1} y^*[n]y[n+d]\mathrm{e}^{-j2\pi\beta n\Delta t}, \quad (14)$$

where d, represents the delay time normalized by the sampling period Δt, and N_y is the total received number of samples. Equation (14) is further used throughout the paper for the graphical representation of the GFDM cyclostationary properties.

As it will be seen later, the cyclostationary properties of both OFDM and GFDM signals are given by the cyclic prefix and useful symbol length. The cyclic prefix construction is graphically presented in Fig. 4 and Fig. 5. In Fig. 4 we have, therefore, represented an example with 3 OFDM symbols. We have also defined $T_{U,OFDM}$ as the useful symbol period, $T_{CP,OFDM}$ as the cyclic prefix period and $T_{S,OFDM} = T_{U,OFDM} + T_{CP,OFDM}$ as the OFDM symbol period.

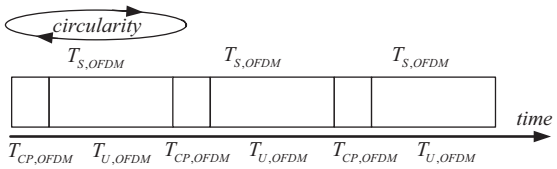

Fig. 4. OFDM structure - example with 3 OFDM symbols

Similar to Fig. 4, in Fig. 5, we have represented a single GFDM symbol with $M = 3$ useful payloads. It can be noticed that the total GFDM symbol period $T_{S,GFDM}$, which consists of a cyclic prefix period $T_{CP,GFDM}$ and a useful symbol

period $T_{U,GFDM}$, can also be expressed in terms of OFDM parameters. The example from Fig. 5 corresponds to a situation where $T_{S,GFDM} = T_{CP,GFDM} + M \cdot T_{U,OFDM}$, with $M = 3$ as mentioned earlier.

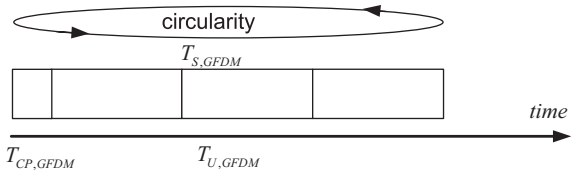

Fig. 5. GFDM structure - example with 1 GFDM symbol and $M = 3$ useful payloads

Further, Fig. 6 shows the CAF of an OFDM signal with $T_{CP,OFDM} = T_{U,OFDM}/4$. Similarly, a GFDM modulation with $T_{CP,GFDM} = T_{U,OFDM}/4$ and $N_s = 16$ is represented in Fig. 7. Please notice that the cyclic frequencies are at multiple of $1/T_{S,OFDM}$ and $1/T_{S,GFDM}$ respectively, and the peaks are encountered at delays equal to $T_{U,OFDM}$ and $T_{U,GFDM}$ respectively.

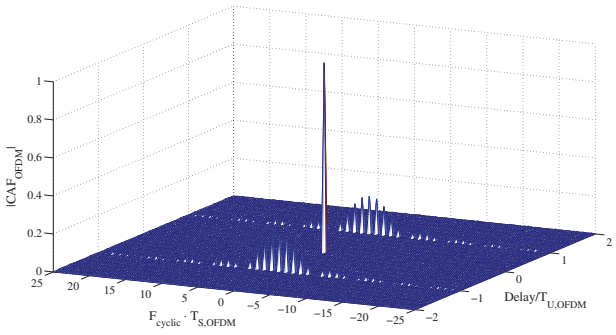

Fig. 6. CAF of OFDM, with $T_{CP,OFDM} = T_{U,OFDM}/4$, (similar as in [14])

However, unlike OFDM, GFDM exhibits extra side crossing peaks, as shown in Fig. 7. In [13], the authors have shown how varying the roll-off factor changes the CAF of GFDM signal. As the roll-off factor is increased, the side peaks in CAF also increase in magnitude. The CAF plots for GFDM have been done on a signal with ICI cancelled out, hence increasing roll-off has no effect on BER performance. An AWGN model with a sigle-path channel is considered here. For multipath channels, the peaks in the CAF will be lower leading to a decrease in detection probabilities, but the overall behaviour of the curves will be similar.

V. Generalized Cyclostationary Detector

The Generalized Likelihood Ratio Test (GLRT) algorithm for cyclostationary detection is computing the covariance matrix given by, $\sum_y(\beta)$, described in detail in [21], [22]. Based on this covariance matrix, the method further computes a test statistic, given as,

$$\mathcal{T} = N_y \cdot \underline{r}_{yy}^{\beta}(\tau) \cdot \sum_{y}^{-1}(\beta) \cdot \underline{r}_{yy}^{\beta}(\tau)^T, \qquad (15)$$

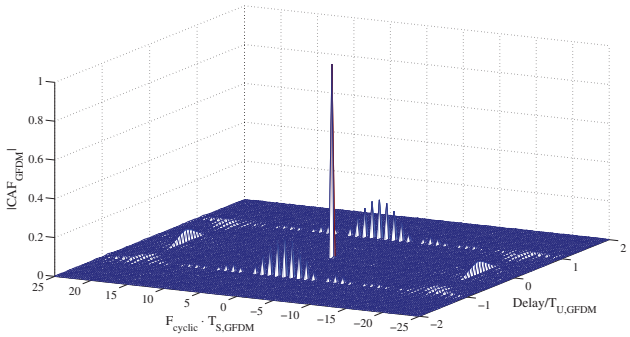

Fig. 7. CAF of GFDM $\hat{y}^{(i)}[n]$ signal, with $T_{CP,GFDM} = T_{U,OFDM}/4$, (similar as in [14])

where, $\underline{r}_{yy}^{\beta}(\tau) = \left[Re\left(R_{yy}^{\beta}(\tau)\right), Im\left(R_{yy}^{\beta}(\tau)\right)\right]$.

The test statistic is then compared with a threshold γ, which is computed with the help of the following equation:

$$P_{FA,target} = 1 - \Gamma(1, \gamma/2), \qquad (16)$$

where Γ is the incomplete gamma function. The threshold γ can be, therefore, expressed as a function of $P_{FA,target}$.

This section also analyzes the effect of different GFDM system parameters (e.g., from Table I) on probability of detection. Moreover, in Fig. 3, we show the variation of BER to length of CP and pulse shaping roll-off factor. We have also shown that, with the implementation of intercarrier interference cancellation, the BER of the GFDM system improves and matches that of theoretical OFDM. Hence, we see that, increasing the roll-off factor increases the BER of an unequalized GFDM system, but that negative influence goes away, once ICI cancellation is implemented. From Fig. 3, we can conclude that increasing the roll-off factor does not affect the BER performance of the GFDM system. As shown in [23], GFDM has really low out of band leakage to adjacent systems. Even with the increase of roll-off factor, the out of band radiation of GFDM is lower than that of OFDM.

TABLE I
GFDM Simulation Parameters

Parameter	Variable	GFDM
Modulation scheme	μ	2 (QPSK)
Samples per symbol	N	512
Subcarriers	K	512
Block size	M	15
Filter Length	L	15
Filter type		RRC
Roll-off factor	α	0.1 to 0.9
Channel Model	h	single-path

In Fig. 8, we have shown the variation of probability of detection to SNR and roll-off factor of the pulse shaping filters. The probability of detection is based on the side peaks which are only evident in GFDM CAF because of the presence of pulse shaping filters. As is evident, with increasing roll-off factor (from 0.1 to 0.9), the probability of detection improves.

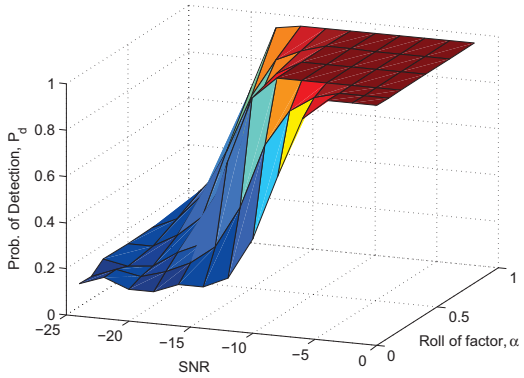

Fig. 8. Probability of detection, P_D, vs. SNR at different roll-off factors, α, with CP $= 1/4$ of the GFDM symbol duration

Extending the work done in [14], [15], the work here shows that improved detection, by increasing the roll-off factor, is not at the cost of bit error rate performance. It is clear that, at a fixed SNR, detection improves with higher the roll-off factor. Also, for a fixed roll-off factor, the detection improves with increasing SNR.

VI. Conclusions

GFDM is a recent multicarrier 5G waveform with flexibility of pulse shaping filters. This reduces the out of band leakage of GFDM to neighbouring adjacent carriers, and hence, makes GFDM very suitable for cognitive radio applications. Cyclostationary detection of a CR signal is an important aspect of spectrum sensing and detection, and this paper extends the work of analyzing cyclostationary properties of GFDM and utilizing them for cyclostationary detection. It has been shown that, with increasing the roll-off factor of the pulse shaping filters, the cyclostationary detection (based on side peaks) increases. It has also been shown that while increasing the roll-off factor might increase the BER of the system, implementation of ICI cancellation schemes mitigates that. So, to get a robust detection performance, with increased roll-off factor, the BER for GFDM systems do not degrade. This robustness of GFDM detection along with low ACLR properties of GFDM make it extremely suitable for CR access in fragmented frequency scenarios.

Acknowledgment

This work has been performed in the framework of the EU-FP7 project ICT-318555 "5GNOW" which is partly funded by the European Union.

References

[1] J. Mitola and Jr. Maguire, G.Q., "Cognitive Radio: Making Software Radios More Personal," *Personal Communications, IEEE*, vol. 6, no. 4, pp. 13–18, 1999.

[2] G. Wunder and et. al, "5GNOW: Non-orthogonal, Asynchronous Waveforms for Future Mobile Applications," *Communications Magazine, IEEE*, vol. 52, no. 2, pp. 97–105, February 2014.

[3] FCC, "Notice of proposed rule-making, in the matter of unlicensed operation in the TV broadcast bands (et docket no. 04-186) and additional spectrum for unli- censed devices below 900 mhz and in the 3 ghz band (et docketno. 02-380)," Tech. Rep. 04-113, FCC, 2004.

[4] D. Noguet, R. Datta, P.H. Lehne, M. Gautier, and G. Fettweis, "TVWS Regulation and QoSMOS Requirements," in *2nd International Conference on Wireless Communication, Vehicular Technology, Information Theory and Aerospace Electronic Systems Technology (Wireless VITAE), 2011*, Feb 2011, pp. 1–5.

[5] G. Fettweis, M. Krondorf, and S. Bittner, "GFDM - Generalized Frequency Division Multiplexing," in *Vehicular Technology Conference, 2009. IEEE 69th*, april 2009.

[6] R. Datta, N. Michailow, M. Lentmaier, and G. Fettweis, "GFDM Interference Cancellation for Flexible Cognitive Radio PHY Design," in *Vehicular Technology Conference (VTC Fall), 2012 IEEE*, Sept 2012, pp. 1–5.

[7] T. Ihalainen, A. Viholainen, T.H. Stitz, and M. Renfors, "Spectrum Monitoring Scheme for Filter Bank Based Cognitive Radios," in *Future Network and Mobile Summit, 2010*, June 2010, pp. 1–9.

[8] T. Ihalainen, T.H. Stitz, and M. Renfors, "Efficient Per-Carrier Channel Equalizer for Filter Bank Based Multicarrier Systems," in *Circuits and Systems, 2005. ISCAS 2005. IEEE International Symposium on*, May 2005, pp. 3175–3178 Vol. 4.

[9] R. Datta, G. Fettweis, Z. Kollar, and P. Horvath, "FBMC and GFDM Interference Cancellation Schemes for Flexible Digital Radio PHY Design," in *Digital System Design (DSD), 2011 14th Euromicro Conference on*, Aug 2011, pp. 335–339.

[10] R. Datta, M. Gautier, V. Berg, Y. Futatsugi, M. Ariyoshi, M. Schuhler, Zs. Kollár, P. Horváth, D. Noguet, and G. Fettweis, "Flexible Multicarrier PHY Design for Cognitive Radio in Whitespace," in *Sixth International ICST Conference on Cognitive Radio Oriented Wireless Networks and Communications (CROWNCOM), 2011*. IEEE, 2011, pp. 141–145.

[11] H. Urkowitz, "Energy Detection of Unknown Deterministic Signals," *Proceedings of the IEEE*, vol. 55, no. 4, pp. 523–531, April 1967.

[12] G. Xu and T. Kailath, "Direction-of-Arrival Estimation via Exploitation of Cyclostationary - A Combination of Temporal and Spatial Processing," *Signal Processing, IEEE Transactions on*, vol. 40, no. 7, pp. 1775–1786, Jul 1992.

[13] S. Enserink and D. Cochran, "A Cyclostationary Feature Detector," in *Signals, Systems and Computers, 1994. 1994 Conference Record of the Twenty-Eighth Asilomar Conference on*, Oct 1994, vol. 2, pp. 806–810 vol.2.

[14] D. Panaitopol, R. Datta, and G. Fettweis, "Cyclostationary Detection of Cognitive Radio Systems Using GFDM Modulation," in *Wireless Communications and Networking Conference (WCNC), 2012 IEEE*, April 2012, pp. 930–934.

[15] R. Datta, D. Panaitopol, and G. Fettweis, "Analysis of Cyclostationary GFDM Signal Properties in Flexible Cognitive Radio," in *Communications and Information Technologies (ISCIT), 2012 International Symposium on*, 2012, pp. 663–667.

[16] E. Conte, A.D. Maio, and G. Ricci, "GLRT-Based Adaptive Detection Algorithms for Range-Spread Targets," *Signal Processing, IEEE Transactions on*, vol. 49, no. 7, pp. 1336–1348, Jul 2001.

[17] F.C. Robey, D.R. Fuhrmann, E.J. Kelly, and R. Nitzberg, "A CFAR Adaptive Matched Filter Detector," *Aerospace and Electronic Systems, IEEE Transactions on*, vol. 28, no. 1, pp. 208–216, Jan 1992.

[18] I. Gaspar, N. Michailow, A. Navarro Caldevilla, E. Ohlmer, S. Krone, and G. Fettweis, "Low Complexity GFDM Receiver Based on Sparse Frequency Domain Processing," in *Vehicular Technology Conference 2013. IEEE 77th*, June 2013, pp. 1 –4.

[19] N. Michailow, R. Datta, S. Krone, M. Lentmaier, and G. Fettweis, "Generalized Frequency Division Multiplexing: A Flexible Multicarrier Modulation Scheme for 5th Generation Cellular Networks," in *German Microwave Conference (GeMiC)*, 2012.

[20] H. Ma and J. Wolf, "On Tail Biting Cconvolutional Codes," *IEEE Transactions on Communications*, vol. 34, no. 2, feb. 1986.

[21] P. Rostaing, T. Pitarque, and E. Thierry, "Performance Analysis of a Statistical Test for Presence of Cyclostationarity in a Noisy Observation," in *Acoustics, Speech, and Signal Processing, 1996. ICASSP-96. Conference Proceedings., 1996 IEEE International Conference on*, May 1996, vol. 5, pp. 2932–2935 vol. 5.

[22] A.V. Dandawate and G.B. Giannakis, "Statistical Tests for Presence of Cyclostationarity," *Signal Processing, IEEE Transactions on*, vol. 42, no. 9, pp. 2355–2369, Sep 1994.

[23] R. Datta and G. Fettweis, "Improved ACLR by Cancellation Carrier Insertion in GFDM Based Cognitive Radios," in *IEEE Vehicular Technology Conference (VTC Spring'14)*, May 2014.